THE ROTATING CONSTRAINED BAR: DERIVATION OF THE GOVERNING EQUATIONS OF MOTION AND NUMERICAL SIMULATIONS

André Fenili, fenili@dem.inpe.br/fenili@unitau.br
National Institute for Space Reserarch (INPE) – Space Mechanics and Control Division (DMC)
Av. dos Astronautas, 1758 – P.O.Box 515, 12201-940 – São José dos Campos, SP, Brazil
and Visiting Professor in University of Taubaté (UNITAU) – Department of Mechanical Engineering
Linear and Nonlinear Vibration Laboratory (Coordinator)
Rua Daniel Danelli s/n (Campus da Juta) – CEP: 12060-440 – Taubaté, SP – Brasil

Alvaro Manoel de Souza Soares, alvaro@unitau.br
University of Taubaté (UNITAU) – Department of Mechanical Engineering and Mechatronics
Rua Daniel Danelli s/n (Campus da Juta) – CEP: 12060-440 – Taubaté, SP – Brasil

João Bosco Gonçalves, jbgoncal@unitau.br
University of Taubaté (UNITAU) – Department of Electrical Engineering
Rua Daniel Danelli s/n (Campus da Juta) – CEP: 12060-440 – Taubaté, SP – Brasil

Abstract. *The mathematical modeling and numerical simulation of constrained dynamic systems is not an easy task when one must take into account the alternance between constrained and unconstrained models. The system investigated in this work is a simplified model for a constrained robot with a rotational joint interacting with an obstructing wall inserted in its workspace. This obstacle, with its own impedance, may also be thought of as an object a robot must handle or interact with. The constraint is introduced in the governing equations of motion via Lagrange multipliers and numerical integrations are performed using the fourth order Runge-Kutta. An expression for the reaction force between the interacting systems is derived. Some numerical simulations are presented in order to remark the special features of such systems.*

Keywords*: constrained dynamics, constrained robot, mathematical modeling, Lagrange multipliers, numerical integration.*

1. INTRODUCTION

The main interest nowadays on studying contact dynamics lies in the investigation of the contact instability problem encountered in robotic manipulators while trying to make contact with an environment, such as grasping or pushing against objects.

In rigid body mechanics, a collision between two bodies is treated as instantaneous, with contact at a single point. Each body is assumed to exert an impulsive force on the other at the point of contact. In the absence of friction the impulse of this force can be easily calculated in terms of a coefficient of restitution. In the presence of friction there are additional difficulties in determining the impulse within the framework of rigid body dynamics (Keller, 1986).

A good literature survey on the subject of contact dynamics can be found in (Gilardi and Sharg, 2002). A general overview of impact analysis and some of the most important approaches in this area can also be found in (Faik and Witteman, 2000).

During contact, it is required that the robot maintains contact with the environment, and also that the impacting forces should not be very high. Then, the goal of any controller is to pass through this transient period successfully, and have the manipulator stably exerting forces on the environment (Mandal and Payandeh, 1995).

The contact dynamics behavior of simulated robotic motion and hence the operational overall performance depends to a large extent on the validity and reliability of the mathematical models considered. Long-term orbital test-beds therefore are needed for contact dynamics model and performance improvement. This will increase the reliability of pre-simulations performed on ground for mission preparation. Flight opportunities for testing are very limited and, besides this, very expensive.

2. GOVERNING EQUATIONS OF MOTION

In physical terms, the system investigated here (and illustrated in Fig. 1) may represent a robot with a rotational joint (the rotating bar as one link of this robot); m_w can be thought as an obstructing wall inserted in the robot's workspace or some object this robot must handle or interact with. In this same sense, M_θ can be thought as an external torque provided by a dc motor.

According to this figure, the free end of the bar is allowed to move along the constraint represented by the mass named m_w. All the movements occur in the horizontal plane. The system is designed in such a way that the bar can turn 360^o but, in a part of its trajectory, contact with m_w is allowed to occur. In the axis passing through point A (perpendicular to the paper sheet), Z, there is a prescribed moment, M_θ, responsible for the turning of the bar.

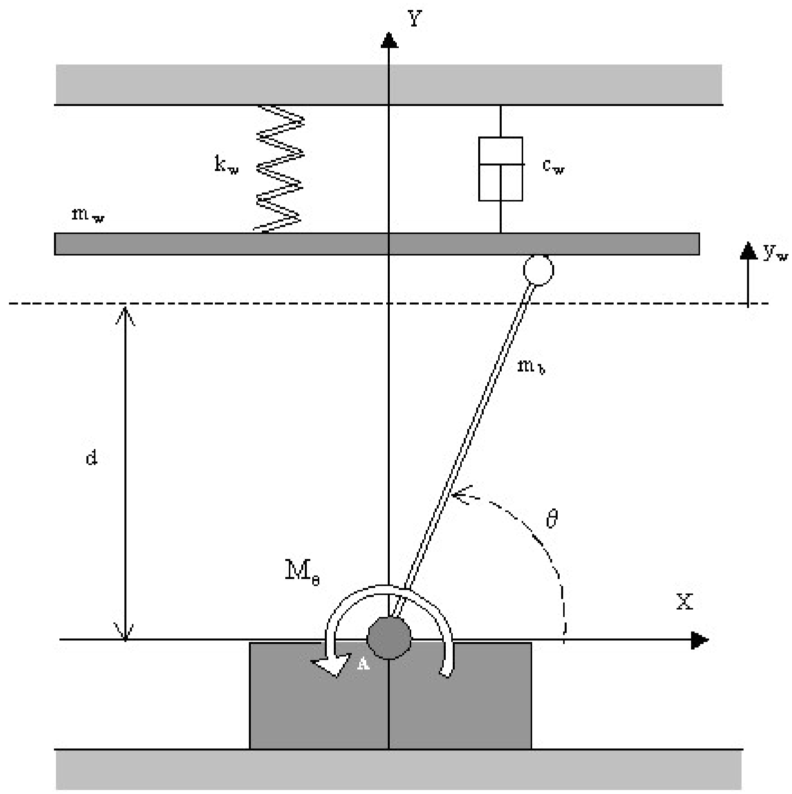

Figure 1. Rotating constrained bar.

The kinetic energy of the system shown in Fig. 1 is given by :

$$T = \frac{1}{2} I_{b,cm} \dot{\theta}^2 + \frac{1}{2} m_b |\dot{r}_{cm}|^2 + \frac{1}{2} m_w |\dot{r}_w|^2 \tag{1}$$

where $I_{b,cm}$ represents the bar moment of inertia around its center of mass, θ represents the bar angular displacement, m_b represents the mass of the bar, $\mathbf{r}_{cm}$ represents the position vector that locates the bar center of mass and $\mathbf{r}_w$ represents the position vector that locates the center of mass of the wall. All the vectors are referenced to the inertial reference frame, XY.

The vectors $\mathbf{r}_{cm}$ and $\mathbf{r}_w$ are given by:

$$r_{cm} = d_{Acmb} \cos\theta\, i + d_{Acmb} \sin\theta\, j \tag{2}$$

$$\mathbf{r}_w = (d + y_w)\mathbf{j} \tag{3}$$

where $\mathbf{i}$ and $\mathbf{j}$ are unit vectors in the X and Y directions, respectively, and d_{Acmb} represents the distance from A to the center of mass of the bar.

Using (2) and (3), the velocities that appear in (1) are given by:

$$\dot{r}_{cm} = -d_{Acmb} \dot{\theta} \sin\theta\, i + d_{Acmb} \dot{\theta} \cos\theta\, j \tag{4}$$

$$\dot{\mathbf{r}}_w = \dot{y}_w \mathbf{j} \tag{5}$$

and, hence:

$$\left|\dot{r}_{cm}\right|^2 = d_{Acmb}^2\dot{\theta}^2 \tag{6}$$

$$\left|\dot{\mathbf{r}}_w\right|^2 = \dot{y}_w^2 \tag{7}$$

Therefore, the kinetic energy given by Eq. (1) can be rewritten as:

$$T = \frac{1}{2}\left(I_{b,cm} + m_b d_{Acmb}^2\right)\dot{\theta}^2 + \frac{1}{2}m_w\dot{y}_w^2 \tag{8}$$

The Rayleigh function that accounts for dissipation of energy associated with the linear damping forces is given by

$$R = \frac{1}{2}c_w\left|\dot{r}_w\right|^2 = \frac{1}{2}c_w\dot{y}_w^2 \tag{9}$$

where c_w represents the damping coefficient associated with m_w. The potential energy is given by

$$V = \frac{1}{2}k_w y_w^2 \tag{10}$$

where k_w represents the stiffness coefficient associated with m_w. The Lagrangian, L, is, therefore, given by :

$$L = T - V = \frac{1}{2}\left(I_{b,cm} + m_b d_{Acmb}^2\right)\dot{\theta}^2 + \frac{1}{2}m_w\dot{y}_w^2 - \frac{1}{2}k_w y_w^2 \tag{11}$$

The Lagrange's equations, considering the constraints to the movement (Rosenberg, 1977; Clough and Penzien, 1975), are given by

$$\frac{d}{dt}\left(\frac{\partial L}{\partial \dot{y}_w}\right) - \frac{\partial L}{\partial y_w} + \frac{\partial R}{\partial \dot{y}_w} = -F_R\frac{\partial r_{fe}}{\partial y_w} \tag{12}$$

$$\frac{d}{dt}\left(\frac{\partial L}{\partial \dot{\theta}}\right) - \frac{\partial L}{\partial \theta} + \frac{\partial R}{\partial \dot{\theta}} = \mathbf{M}_\theta + F_R\frac{\partial r_{fe}}{\partial \theta} \tag{13}$$

where $\mathbf{F}_R$ is a vector representing the reaction force related to the interaction between the rotating bar and the constrained surface (m_w and the compliance associated to it). The reaction force is considered in this work only through its normal component, $F_N\boldsymbol{\nabla}\boldsymbol{\Phi}$, with $\mathbf{F}_N$ representing the amplitude of the normal force. The normal (reaction) force is applied in the contact point between the tip of the rotating bar and m_w and is represented normal to the constarined surface, pointing in the direction –Y (see Fig. 1). No friction force (tangential force component) is considered. The absence of friction forces in this problem is an ideal assumption. This first approach must be improved in the future. In real applications, the absence of friction is hardly found in mechanical systems. This condition can be approximately obtained in a prototype of the dynamic system presented here, for instance, by the burnishing of the contacting surfaces (although that there will be still some neglegible friction). The vector $\mathbf{r}_{fe}$ locates the free end of the bar. The quantity $\boldsymbol{\Phi}$ represents the equation of the constrained surface given by

$$\boldsymbol{\Phi} = d + y_w - Y = 0 \tag{14}$$

and $\boldsymbol{\nabla\Phi} = \frac{\partial\Phi}{\partial X}\mathbf{i} + \frac{\partial\Phi}{\partial Y}\mathbf{j}$. The position of the free end of the bar is given by

$$r_{fe} = \ell\cos\theta\, i + \ell\sin\theta\, j \tag{15}$$

or

$$r_{fe} = \ell\cos\theta\, i + (d + y_w)\, j \tag{16}$$

where ℓ represents the total length of the bar. The term $\frac{\partial \mathbf{r}_{fe}}{\partial \alpha}$ (where $\alpha = y_w$ or θ) represents a vector that accounts for the variation of the free end position related to each one of the generalized coordinates considered. This variation is associated with "the work developed by the constraint forces".

Applying Lagrange's equations (Eq. (12) and Eq. (13)) the governing equations of motion are given by

$$m_w \ddot{y}_w + c_w \dot{y}_w + k_w y_w - F_N = 0 \tag{17}$$

$$(I_{b,cm} + m_b d^2_{Acmb})\ddot{\theta} + F_N \ell\cos\theta = M_\theta \tag{18}$$

The equation for the beginning of contact is given by:

$$d + y_w - \ell\sin\theta = 0 \tag{19}$$

Equation (17) represents the governing equation of motion for the generalized coordinate y_w, and Eq. (18) represents the governing equation of motion for the generalized coordinate θ. Together with these equations, Eq. (19) represents an additional relationship between the generalized coordinates θ and y_w when contact occurs. This set provides three equations and three unknowns (θ, y_w and F_N) considering the constrained problem and two equations and two unknowns (θ and y_w) considering the unconstrained problem (with $F_N = 0$).

In contact condition, for this problem, there is the loss of one degree of freedom. In other words, one of the variables is dependent of the other and the constrained equation of motion can be given by:

$$\begin{aligned}&(I_{b,cm} + m_b d^2_{Acmb} + m_w \ell^2\cos^2\theta)\ddot{\theta} - m_w \ell^2\dot{\theta}^2\sin\theta\cos\theta + c_w \ell^2\dot{\theta}\cos^2\theta + \\ &k_w \ell^2\sin\theta\cos\theta - k_w d\ell\cos\theta = M_\theta\end{aligned} \tag{20}$$

It is initially assumed that e = 0 (where e is the coefficient of restitution), i.e. fully plastic impact. Separation will take place when the normal force is zero. Otherwise, for any other value of the coefficient of restitution, it is possible to occur multiple impacts.

3. THE CONTACT (NORMAL) FORCE

The time behavior of the reaction force, F_N, is given by:

$$\begin{aligned}F_N = &\frac{m_w \ell\cos\theta}{I_{b,cm} + m_b d^2_{Acmb} + m_w \ell^2\cos^2\theta}\Big(M_\theta + m_w \ell^2\dot{\theta}^2\sin\theta\cos\theta - c_w \ell^2\dot{\theta}\cos^2\theta - \\ &k_w \ell^2\sin\theta\cos\theta + k_w d\ell\cos\theta \Big) - m_w \ell\dot{\theta}^2\sin\theta + c_w \ell\dot{\theta}\cos\theta + k_w \ell\sin\theta - k_w d\end{aligned} \tag{21}$$

It is evident that F_N depends on the impacting body velocities ($\dot{\theta}$) but also on the material properties of the body posed as constraint (m_w, k_w and c_w).

Two different set of governing equations of motion must be integrated to cover all the system dynamics. One of these sets is always generating the states for the other. The necessity for changing from one set of governing equations to another represents a source of integration errors, since the integrator is faced with singularities.

The problem presented in this paper and the procedures developed for its analysis are general and can be extended to many other problems.

4. NUMERICAL SIMULATIONS

Three different cases are considered by changing two of the system parameters. The set of parameters considered in each case is presented in Tab. 1.

In all the results presented here, m_w starts in the rest position. Friction forces are not considered here. Multiple impacts are allowed to occur. Depending on system parameters, in the same time interval and considering the same excitation, a different number of colisions can be detected. In the results presented here, for example, in cases 1 and 2 four colisions are detected while in case 3 five colisions are detected.

The external torque, M_θ, is constant and equal to 5.0 Nm. The length of the bar is 1.0 m. The distance d (see Fig.1) is equal to 0.6m.

The numerical integrator used is the fourth order Runge-Kutta with time step of 0.0001 s.

Table 1. Parameters considered for the numerical simulations.

Cases considered	k_w (kg/s^2)	c_w (kg/s)	m_w (kg)	m_b (kg)
case 1	50.0	10.0	2.0	2.0
case 2	100.0	10.0	2.0	2.0
case 3	100.0	20.0	2.0	2.0

The basic idea here is to compare case 1 with case 2 and case 2 with case 3. From case 1 to case 2 there is an increasing in the constraint stiffness and from case 2 to case 3 there is an increasing in the constraint damping. The following figures illustrate the results for each one of the three cases considered.

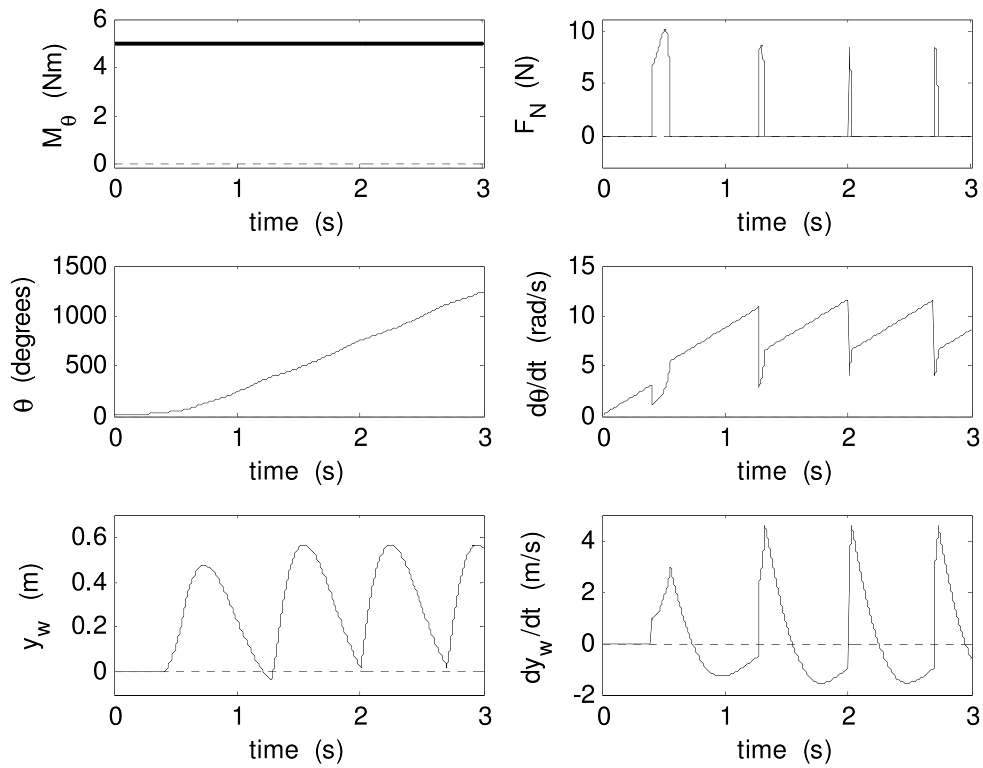

Figure 2. Results for Case 1.

As can be seen when comparing F_N from Fig. 2 with F_N from Fig. 3, by increasing the value of k_w form 50 kg/s^2 to 100 kg/s^2 the amplitude of the contact force (normal component only since friction forces are not considered here) increases for the first impact mainly. The same effect is observed when comparing F_N from Fig. 2 with F_N from Fig. 3.

It is evident in the velocity curves for $\dot{\theta}$ and $\dot{y}_w$ the singulatities (jumps) that takes place in the moment the bodies impact each other. This phenomena might be a source of integration errors. In this sense, the time step considered is of great importance for convergence of the solution and the results obtained.

As shown in Figs. 2 to 4, the value of the contact force at the instant contact is stabilised (impact) is not necessarily the higher value for F_N. As seen in Eq. 21, the contact (normal) force depends on system parameters and states (θ and $\dot{\theta}$) and some of these parameters and all the states involved are varying with time. In this sense, it is not so obvious the time behaviour of this force.

When the distance between the masses goes to zero, the masses maintain the contact for some time. As stated before in this same text, in the analyses developed here one considers the coefficient of restitution equal to zero.

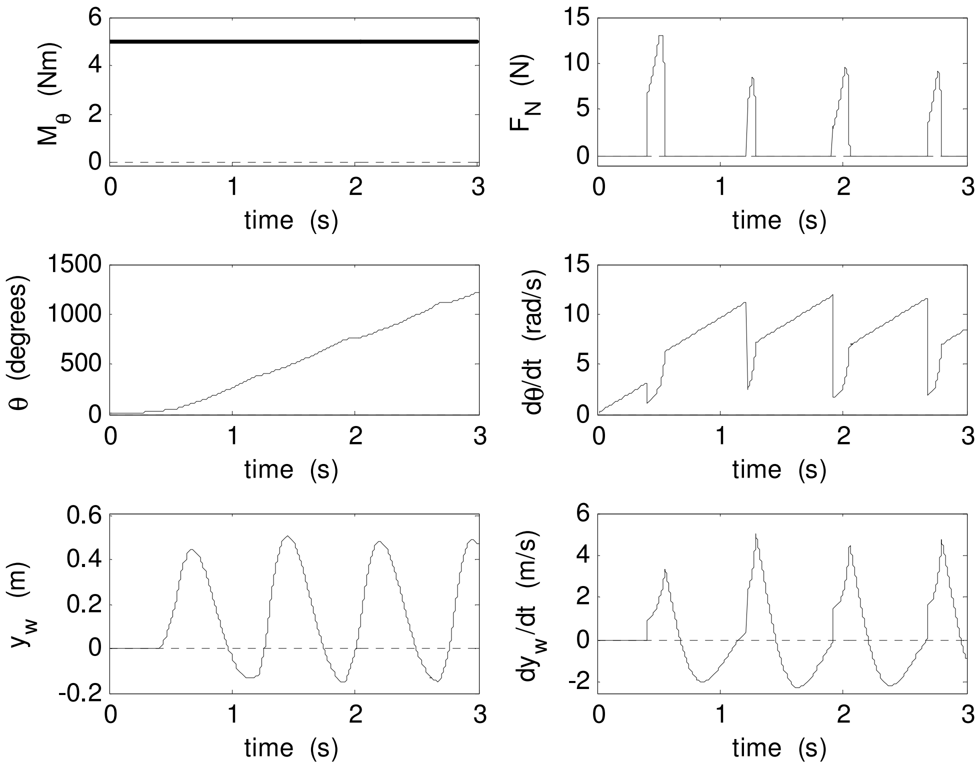

Figure 3. Results for Case 2.

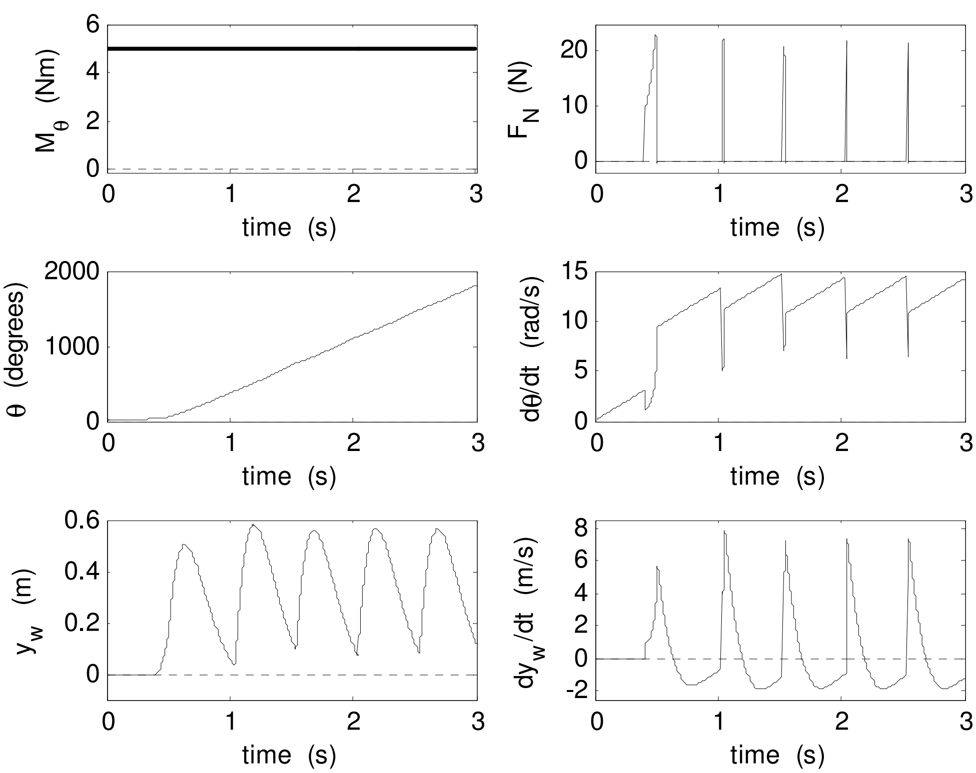

Figure 4. Results for Case 3.

The numerical simulations show that the first impact presents the higher amplitude for F_N than the subsequent ones.

The dashed horizontal line in Fig. 1 represents the rest position of m_w. The displacement of m_w taken above this line is positive for this mass and the displacement taken below this line is negative. In case 1, m_w crosses this line just once (Fig. 2). In case 3, this line is never crossed (Fig. 4). In case 2, this line is crossed many times (Fig. 3). When impact with the tip of the bar occurs, m_w changes the direction of its moviment.

The bar is pinned in point A (see Fig. 1) and, therefore, the frequency of the impacts (or the number of impacts released) as well as its duration is closely related to the properties of m_w (including the compliance given by k_w and c_w). However, the properties of the bar, the states of both bodies and the torques involved (M_θ) have also some influence in the number of impacts. For example: considering the same time interval, if M_θ increases the angular displacement of the bar increases and the number of contacts increases. By changing k_w or c_w, for example, one modifies the frequency of the unconstrained m_w and, therefore, the number of times this mass is in the region into which impacts may occur. When the bodies separate, a different (from the constrained) dynamical behaviour is developed by each one of the bodies.

5. CONCLUSIONS

Regarding the mathematical model presented for F_N (the normal component of the contact force developed between the colliding bodies), one of the main results of this investigation up to this point is the verification of the dependence of this force on the colliding bodies physical parameters and states. A poor knowledge of these quantities may result in a weak knowledge of the real system under investigation. It is hard (or impossible) sometimes to measure the constraint compliance – stiffness and damping. It means that some kind of identification or estimation of parameters must be carried through sooner or later by the analyst in order to have sufficient knowledge about and properly control such systems.

6. ACKNOWLEDGEMENTS

The authors wish to thank CNPq – Conselho Nacional de Desenvolvimento Científico e Tecnológico (National Counsel of Technological and Scientific Development) for the grants that supported this study.

7. REFERENCES

Clough, R. W. and Penzien, J., 1975, “Dynamics of Structures”, McGraw-Hill Kogakusha Ltd., Tokio, Japan.

Faik S. and Witteman, H., 2000, “Modeling of impact dynamics: a literature survey,” 2000 International ADAMS User Conference.

Gilardi, G. and Sharf, I., 2002, “Literature survey of contact dynamics modeling”, Mechanisms and Machine Theory.

Keller, J. B., 1986, “Impact with friction”, Journal of Applied Mechanics, vol. 53, pp. 1-4, March.

Mandal, N. and Payandeh, S., 1995, “Control strategies for robotic contact tasks: an experimental study”, Journal of Robotic Systems, 12 (1), pp. 67-92.

Rosenberg, R. M., 1977, “Analytical Dynamics of Discrete Systems”, Plenum Press, New York.

8. RESPONSIBILITY NOTICE

The authors are the only responsible for the printed material included in this paper.